REPORT DOCUMENTATION PAGE

Form Approved
OMB No. 0704-0188

1. REPORT DATE *(DD-MM-YYYY)*	2. REPORT TYPE	3. DATES COVERED *(From - To)*
20032006	Journal Article	

4. TITLE AND SUBTITLE

An Acoustic-Instrumented Mine for Studying Subsequent Burial

5a. CONTRACT NUMBER

5b. GRANT NUMBER

5c. PROGRAM ELEMENT NUMBER

6. AUTHOR(S)

John Bradley, Sean Griffin, Maurice Thiele, Jr., Michael D. Richardson, Peter D. Thorne

5d. PROJECT NUMBER

5e. TASK NUMBER

5f. WORK UNIT NUMBER

7. PERFORMING ORGANIZATION NAME(S) AND ADDRESS(ES)

Naval Research Laboratory
Marine Geoacoustics Division
Stennis Space Center, MS 39529

8. PERFORMING ORGANIZATION REPORT NUMBER

NRL/JA/7430-06-9

9. SPONSORING/MONITORING AGENCY NAME(S) AND ADDRESS(ES)

Office of Naval Research
800 North Quincy Street
Arlington VA 22217-5000

10. SPONSOR/MONITOR'S ACRONYM(S)

ONR

11. SPONSOR/MONITOR'S REPORT NUMBER(S)

12. DISTRIBUTION/AVAILABILITY STATEMENT

Approved for public release; distribution is unlimited

13. SUPPLEMENTARY NOTES

IEEE Journal of Oceanic engineering, Vol. 32, No. 1 January 2007

14. ABSTRACT

Abstract—**The U.S. Navy is supporting the research to develop and validate stochastic, time-dependent, mine burial prediction models to aid the tactical decision making process. This research requires continuous monitoring of both mine behavior during burial, and the near-field processes responsible for burial. A new instrumented mine has been developed that far exceeds the capabilities of the earlier optically instrumented mine in terms of the burial processes that can be measured. The acoustic-instrumented mine (AIM) utilizes acoustic transducers to measure burial and scour, localized flow rates, and sediment size and concentration in**

15. SUBJECT TERMS

Acoustic transducer, instrumented mine, mine burial, scour

16. SECURITY CLASSIFICATION OF:			17. LIMITATION OF ABSTRACT	18. NUMBER OF PAGES	19a. NAME OF RESPONSIBLE PERSON
a. REPORT	b. ABSTRACT	c. THIS PAGE			Michael Richardson
Unclassified	Unclassified	Unclassified	UU	14	19b. TELEPHONE NUMBER *(Include area code)* 228-688-4621

An Acoustic-Instrumented Mine for Studying Subsequent Burial

John Bradley, Sean Griffin, Maurice Thiele, Jr., Michael D. Richardson, and Peter D. Thorne

Abstract—**The U.S. Navy is supporting the research to develop and validate stochastic, time-dependent, mine burial prediction models to aid the tactical decision making process. This research requires continuous monitoring of both mine behavior during burial, and the near-field processes responsible for burial. A new instrumented mine has been developed that far exceeds the capabilities of the earlier optically instrumented mine in terms of the burial processes that can be measured. The acoustic-instrumented mine (AIM) utilizes acoustic transducers to measure burial and scour, localized flow rates, and sediment size and concentration in the water column. The AIM also includes sensors for measuring mine orientation and movement, as well as oceanographic information such as significant waveheights, wave period, and water temperature. Four AIMs were constructed and deployed during the Indian Rocks Beach (IRB, FL) and Martha's Vineyard Coastal Observatory (MVCO, Edgartown, MA) mine burial experiments. The results from the field experiments have proven that the sensor suite is viable in providing a wealth of data that are critical in understanding and modeling the complex subsequent burial process.**

Index Terms—**Acoustic transducer, instrumented mine, mine burial, scour.**

I. Introduction and History

MINING has proven to be an effective and economical means of both offensive and defensive warfare [1], [2]. Nearly every conflict since the Revolutionary War has seen the use of mines and they remain a probable weapon for any future conflicts. Mines are simple to build and deploy with very little risk but require sophisticated equipment to locate and significant cost and risk to counter. "In short, there is superior economy of force in the use of these weapons . . . "[1].

One of the difficulties in mine countermeasures operations is the detection and classification of buried mines. Bottom mines are easily buried by scour from wave action or tidal currents, wave-induced liquefaction, migrating sand dunes, or changes in seafloor morphology. These subsequent burial processes are dependant on sediment type, depth, meteorological conditions and history, wave action, bottom currents, and mine properties (density, size, and shape) [3]. Once buried, sonar detection is difficult, especially at the long standoff distances required for mine hunting ships. Prediction of mine burial is also a critical input to tactical decision aids that determine sonar effectiveness, rates of clearance, or whether to hunt, sweep, or avoid an area. The U.S. Navy is thus interested in studying and modeling the burial process to improve naval tactical decision aids.

Early work on subsequent mine burial used noninstrumented mine shapes which required diver observations and were subjective, expensive, and limited by diver availability. Especially problematic was the limited visibility and difficult logistics during storm events, when burial is most active. Forschungsanstalt der Bundeswehr für Wasserschall und Geophysik (FWG, Kiel, Germany) and much later Omni Technologies Inc. (OTI, New Orleans, LA) and the U.S. Naval Research Laboratory (NRL, Stennis Space Center, MS) developed self-recording mines that use optical methods to record the mine burial state [4], [5]. The OTI/NRL mine improved on the FWG instrumented mine design by adding sensors that record changes in mine heading, roll, and pitch which are critical to the study of mine burial. Optical techniques have several drawbacks however, such as sensor fouling from marine growth and the hydrodynamic effects on flow of the protuberances on the mine surface possibly enhancing mine burial. Neither of the early instrumented mine types has sensors to measure near-field processes responsible for burial but, notwithstanding, research using these mines has provided significant understanding of mine burial processes [4]–[6].

II. Improved Subsequent Burial Instrumented Mine

A. Background

OTI and NRL have developed a new generation of subsequent burial instrumented mines that far exceed the capabilities of previous systems [7]. These bronze cylindrical instrumented mines use acoustic sensors mounted flush with the mine surface to measure burial and scour (Fig. 1). The acoustic burial sensors provide increased coverage from earlier versions (112 versus 72 point sensors). As with the early NRL/OTI, optical instrumented mine, roll, pitch, and heading are measured with accelerometers and an electronic compass. Accelerometers (three-axes) are used to detect mine motion that occurs when the mine falls into scour pits or the seafloor liquefies. Pressure sensors have been added to measure bottom pressure fluctuations associated with tidal changes and surface gravity waves. Added hydrophones can be used to support fleet mine hunting exercises and can also be used as an acoustic locator which responds when interrogated with a coded pulse. Coherent acoustic Doppler sensors have

Manuscript received July 21, 2005; revised February 10, 2006; accepted March 20, 2006. Building of the four AIMs was supported by the U.S. Office of Naval Research under Contracts N00014-00-C-0431 and N00014-01-C-0055, by the U.S. Naval Research Laboratory under Contract N00014-97-C-6001, and by the Naval Sea Systems Command (NAVSEA) Small Business Innovation Research (SBIR) Award under Contract N00024-01-C-4039.

Guest Editor: R. H. Wilkens.

J. Bradley, S. Griffin, and M. Thiele, Jr. are with the Omni Technologies, Inc., New Orleans, LA 70124 USA (e-mail: jbradley@otiengineering.com).

M. D. Richardson is with the Marine Geosciences Division, U.S. Naval Research Laboratory, Stennis Space Center, MS 39529 USA (e-mail: mike.Richardson@nrlssc.navy.mil).

P. D. Thorne is with the Proudman Oceanographic Laboratory, Liverpool L3 5DA, U.K. (e-mail: pdt@pol.ac.uk).

Digital Object Identifier 10.1109/JOE.2007.890945

Fig. 1. Acoustic-instrumented mine.

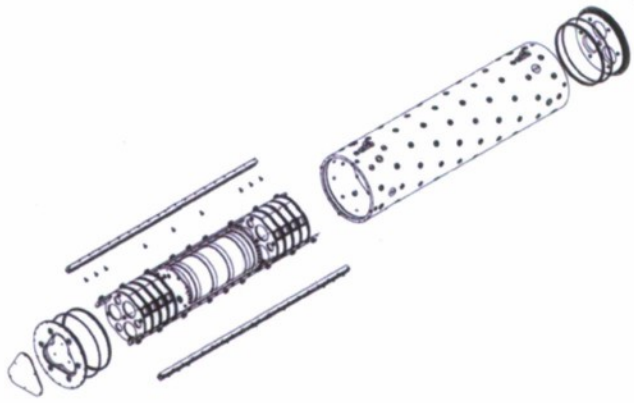

Fig. 2. Instrumented mine internal assembly.

been developed to measure hydrodynamic flow rates around the mine. Calculated flow rates (mean and instantaneous) from the Doppler sensors and sediment concentration values calculated from the acoustic backscatter (ABS) of the burial sensors can be used to estimate rates of the sediment transport. Temperature is logged for use in acoustic calculations. Sufficient data storage space and power is available for a one-year deployment. The design of the mine allows it to be tethered to a shore-based station for near-real-time data collection. During nontethered deployments, the data are offloaded after the mine has been recovered.

B. Mechanical Overview

The instrumented mines are cylindrically shaped (2.033 m long and 0.533 m in diameter), weigh approximately 800 kg fully loaded, and have an average density of 1760 kg m^{-3}. A naval marine bronze was selected for the housing because of its high-density, nonmagnetic, antifouling, and corrosion resistant properties. These mines have 135 penetrations for sensors and connections all designed to be flush to the housing to reduce localized scour due to turbulent flow around protrusions.

Inside the mine shape, an inner frame is used to support the electronics and battery packs (Fig. 2). A roller system allows the 130-kg frame to be easily and safely inserted and extracted for servicing. The battery packs are located on each end of the frame to balance the load. At the center of the inner frame is a second pressure housing protecting the majority of the mine's electronics and storage media in case the watertight integrity of the outer housing fails. All external electrical connectors are recessed on the front end-cap and covered with a bronze plate maintaining the mine's smooth outer surface.

C. Electronics Overview

The acquisition electronics package was designed for flexibility and simplicity. Two relay boards external to the electronics canister act as wiring centers for all the sensors, thus reducing the number of wires attached directly to the acquisition system. The purpose of the acquisition system is to select the active sensor, acquire data, and store that data to disk. Each sensor group in the system is controlled by its own subsystem. Each subsystem has its own microprocessor that is responsible for sampling the related sensor and storing the data to a temporary storage cache. Whenever this cache fills up, a single board computer running the Linux operating system is powered on and the data are transferred to one of four 20-GB hard drives. Each time the storage computer is powered on, a different hard drive is selected to provide redundancy in the event of a drive failure. To conserve battery power, each subsystem is powered only when data are being acquired from a selected sensor. A control system board which is continuously on, is used to turn each subsystem on and off according to a mission profile which is downloaded from the topside software interface.

D. Power Supply

Up to eight cylindrical alkaline D-cell battery packs, each weighing 16.5 kg, provide power for the mine. Battery packs are used in even multiples to provide redundant power and balance the mine's weight. The eight battery packs can provide up to 365 days of energy depending upon the deployment scenario. The battery packs have a starting voltage of 12.8 V (eight D-cells in series) when new and the system can operate normally until the voltage falls below 6.5 V. Each cylindrical battery pack uses 72 alkaline D-cells that are spot-welded together with tin strips in an electrical arrangement of nine parallel sets of eight series D-cells. If eight battery packs are used then there are 72 parallel sets of eight series D-cells available. D-cells were selected based on a beneficial cost to energy density ratio, ready availability, safety and ease of disposal.

III. Sensor Suite

A. Burial Sensors

The burial sensors are unique and are more functional than the name implies. These transducers are designed to determine the burial state at each of the 112 transducer locations, allowing percent system burial to be computed. Analysis of acoustic returns also allows characterization of changing geometric dimensions of the surrounding scour pit, detection of bedload transport, and estimation of suspended sediment size and concentration. Burial transducer signals might also be processed using coherent Doppler flow techniques to provide high-resolution flow

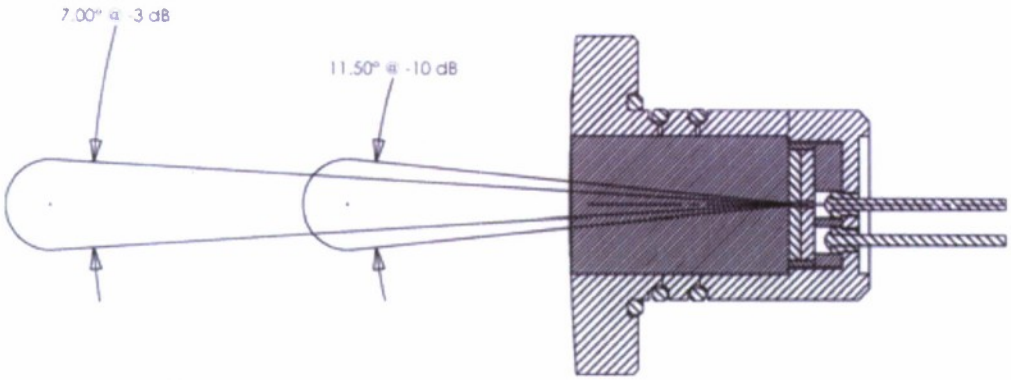

Fig. 3. Burial transducer cross-sectional view and beam pattern.

measurements over the entire mine surface, though this function is not currently implemented. The 112 burial transducers are distributed evenly across the surface of the mine with six sensors in each end cap and ten sensor rings with ten sensors per ring evenly covering the cylinder surface.

The burial transducer design includes a recessed piezoceramic element potted in urethane (Fig. 3). The ceramic element is 2.54 cm away from the transducer face which is flush with the outer mine surface. Urethane, with an acoustic impedance similar to water, provides an almost acoustically transparent interface when immersed in seawater. A strong reflection from the transducer face therefore indicates sediment flush with the mine surface (i.e., the mine surface is buried). The 2.54-cm thickness of the urethane provides sufficient two-way travel time (33.9μs) from the ceramic element to the transducer face to allow the transmit pulse width and transducer ring down time to reach an acceptable point before any possible echo from the transducer face occurs.

In the burial sensor system, the transmit pulse has a width of less than 10.67 μs (either at 1.5 or 3.0 MHz). The input of the receiver is clamped to ground before each transmit pulse and is released 26.67 μs after the start of the transmit pulse. The transmit pulse envelope and its carrier signal are synchronized to the sample rate of the receiver's analog-to-digital (A/D) converter.

The receiver uses a quadrature demodulation technique that produces two quadrature outputs from the local oscillators operating at the same frequency as the transmit pulse carrier. These quadrature outputs are mixed with the receive signal to produce an in-phase (I) signal and quadrature (Q) signal that are basebanded and centered about the direct current (dc). The I and Q mixer outputs are filtered and routed to a stereo, delta–sigma, A/D converter and sampled at a rate of 93 750 Hz. The receiver system stores the digitized 16-b output word pairs for each I and Q channel output sample and the magnitude (M) of each sample pair is calculated according to $M = \sqrt{I^2 + Q^2}$.

The receiver system stores 125 sample pairs for each transmit session. The 10.67-μs time interval between receiver sample represents a delta range of 0.8 cm. In the receive data, the first five samples can be used to measure the ambient ocean noise. A receiver clamp circuit activates between the sixth and seventh sample and the transmit pulse starts between the ninth and tenth

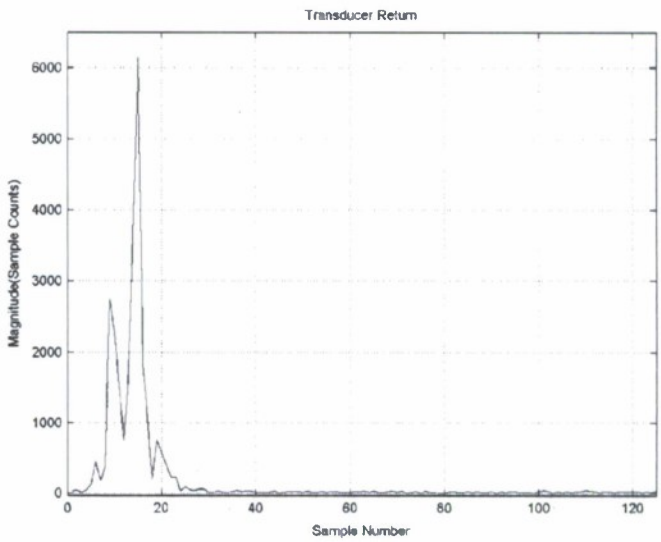

Fig. 4. Burial transducer reflection magnitude.

sample. During the 12th sample, the receiver clamp circuit releases and the echo from the urethane/water interface occurs at the 13th sample. The 125th sample occurs at a range of 0.92 m from the face of the transducer element. A typical magnitude plot of the ping return (Fig. 4) will show a peak between samples nine and ten that indicates the clamped outgoing pulse and another peak at sample 13 that indicates an echo from the transducer face.

Determination of which sensors are buried below the sediment-water interface is performed in postprocessing. Impedance differences usually occur when sediment or water covers a transducer face. This causes acoustic reflection differences (at a range of 2.54 cm) for buried or unburied conditions. Postprocessing allows the user to refine calculated sensor burial conditions using information from all sensor locations. Signal averaging is also possible, which improves the signal-to-noise ratio (SNR) and thus burial detection performance. Intervals between sampling events (using all 112 burial transducers) can be as short as 30 min.

Suspended sediment concentration and size distribution are measured from water-column backscatter strengths using the

burial transducers. This technique requires multifrequency signals and thus the need for both 1.5- and 3.0-MHz burial transducers. Thorne *et al.* provide a thorough description of these techniques and the methods of transducer calibration [8].

The initiation of bedload transport can also be estimated using correlation techniques applied to the successive backscatter returns from the sediment surface. When bedload transport begins, a change in phase of the returned waveforms is expected as a result of changing fine scale seafloor roughness (i.e., the grains begin to move).

B. Flow Sensors

Two different flow sensor designs, both based on coherent acoustic Doppler techniques, are used to measure flow around the mine. The coherent acoustic Doppler technique uses a pair of transmit pulses to determine two echo phase values of a reflector at a designated range. At each designated range the reflector's in-line velocity is equal to the echo phase difference of the reflector divided by the time interval between the transmit pulses. If the reflector is stationary, the phase of each echo should be the same, whereas any inline motion of the reflector between transmit pulses will cause the phase of each echo to be different.

The coherent acoustic Doppler technique requires the same quadrature demodulation technique utilized for the burial transducers. The phase of the echo at each designated range is calculated according to $\tan^{-1}(Q/I)$. It is essential that the transmit pulse, including the carrier frequency, be synchronized with the A/D converter sampling to ensure that reflector phase differences at a designated range are accurate. Each designated range is represented by a fixed number of samples after each transmit pulse. To avoid ambiguous results, the total phase difference between two echoes at a designated range must be less than $+/-180°$. This criterion places constraints on the range of reflector velocities, the carrier frequency of the transmit pulse, and the time interval between transmit pulses.

The first flow sensor, an acoustic Doppler current profiler (ADCP), operates at 1.5 MHz with three elements per sensor placed in a 2.9-cm-diameter circle, 120° apart (Fig. 5). The elements incline inward at 30° angles and are recessed from the face of the transducer by 2 cm. The beam centers of each element cross approximately 2.5 cm above the transducer face. Measurement range of the ADCP is approximately 1 m from the transducer face. Since each element will provide a flow rate along its axis, geometric relationships can be used to obtain a 3-D flow description relative to the axis of the mine. Three ADCP sensors are placed at 120° intervals around the circumference of the mine near each end cap for a total of six ADCPs.

The second flow sensor is a single-element 500-kHz transducer and it is designated as the Doppler flow sensor. Six of these Doppler flow sensors are located on the mine: one on each end cap and four around the center of the mine cylinder, 90° apart. Data acquisition and processing is identical to that of each ADCP channel. Because these are single-element units with beams directed radially outward from the center of the mine, only the flow normal to the transducer center axis is calculated.

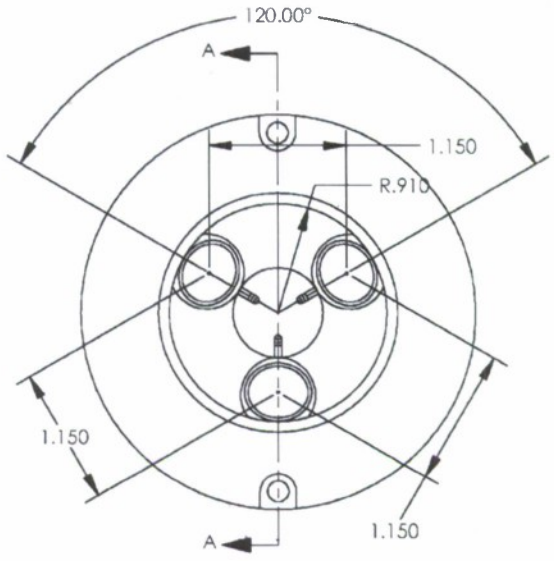

Fig. 5. ADCP transducer piezoceramic element configuration (dimensions in inches).

The flow measurements are obviously important for monitoring bottom currents and turbulent flow induced by the presence of the mine but also for calculating sediment flux in and out of the scour pit when combined with the suspended sediment measurements. This provides a direct measure of the sediment volume moving in the mine's vicinity during storm events or during tidal cycles.

C. Orientation Sensors

Orientation measurements are critical to the analysis of subsequent mine burial processes. Motion before, during, and after storm events provides insight into the burial process. Burial, hydrophone, and flow sensors also require orientation information to compare successive measurements for transformations to a common coordinate system.

The instrumented mine orientation sensor consists of a commercial off-the-shelf, three-axes, fluxgate compass and three-axes accelerometer for roll and pitch measurements. Heading accuracy is on the order of $\pm 2.0°$ and roll and pitch accuracy is approximately $\pm 0.5°$. The selection of a nonmagnetic housing allows use of a magnetic heading sensor as opposed to a fiber-optic compass. Sensor sampling intervals are selectable and can be made as fast as the fastest sampling interval of the other sensors.

D. Pressure Sensors

Six pressure sensors monitor changes in mean water depth (primarily tidal), significant waveheight, and period. These transducers have a range of 0–100 lb/in^3, giving a maximum measurable water depth of approximately 45 m with a sensitivity of approximately 1 mm. Pressure sensor measurements are programmed to occur at user selectable intervals and durations (e.g., for 15 min every hour). Each pressure transducer is sampled at ten samples per second for the duration of each sample set. The raw pressure data are stored after each sample

set and the surface wave statistics are computed during postprocessing. Knowledge of surface wave conditions are required as an input to most scour and liquefaction mine burial models. During postprocessing, the raw pressure data stored by the mine are used to calculate significant waveheight, average wave period, and tide.

E. Hydrophones

Hydrophones are used to measure acoustic energy impinging on the mine's surface from search and classification sonars. Combined with the instrumented mine's burial and orientation measurements, this information is useful for postmission analysis of military training exercises. The hydrophones also have the capability of responding to a coded pulse to determine mine health and location as well as for responding to search sonars during training exercises; however, this feature is currently not implemented. It is envisioned that acoustic modems could be used on each mine to construct an intelligent minefield for fleet exercises. The hydrophones are capable of receiving acoustic energy from 10 to 100 kHz. The sampling method, however, band-limits the signal to a user-selected 10-kHz band located within the transducer's range. The hydrophones are monitored continuously for energy 20 dB (or other selected power level) above background noise. This triggers a storage event in which both pretrigger and post-trigger data (16-b I and Q samples) are stored for all six hydrophones.

F. Accelerometers

A $\pm$2-g-rated, three-axes accelerometer is used to continuously monitor acceleration. Accelerations associated with mine movement such as rocking and falling into scour pits and sinking during liquefaction can be detected. These sensors are located near the geometric center of the mine and mine movement associated with accelerations greater than 0.1 g will trigger a storage sequence whereby pretrigger and post-trigger accelerations are sampled and stored. The continuously monitored accelerometer provides immediate detection of motion that would normally be missed by periodic orientation measurements. Each accelerometer axis is sampled at 2929 samples per second.

IV. Experiment Results

Four AIMs were fabricated and deployed as part of two mine burial experiments. The first experimental site was off Indian Rocks Beach (IRB) near Tampa, FL, from January 8 to March 15, 2003. Martha's Vineyard Coastal Observatory (MVCO, Edgartown, MA) was the second experimental site from October 1, 2003 to April 16, 2004. Each AIM was fabricated with different sensor capabilities in terms of the ABS and flow transducers (Table I). AIMs 2 and 3 were fitted with four Doppler transducers while AIM4 was fitted with six ADCP transducers. On AIMs 3 and 4, 12 burial transducers on the top side of the mine housing were replaced with ABS transducers used for detecting suspended sediments and calculating sediment concentration and transport. These transducers can carry out their function until the AIM rotates to an angle that moves their beams out of the water column and into the sediment.

TABLE I
Acoustic Configuration for Each AIM

	Burial	Backscatter	Doppler	ADCP
AIM1	Installed	None	None	None
AIM2	Installed	None	Installed	None
AIM3	Installed	Installed	Installed	None
AIM4	Installed	Installed	None	Installed

TABLE II
R^2 Statistics for AIM Versus AIM and AIM Versus WHOI Significant Waveheight Calculations

Comparison	R^2 Statistic
AIM1 - AIM3	0.9519
AIM1 - AIM4	0.9652
AIM3 - AIM4	0.9812
AIM1 - WHOI	0.9276
AIM3 - WHOI	0.9051
AIM4 - WHOI	0.9214

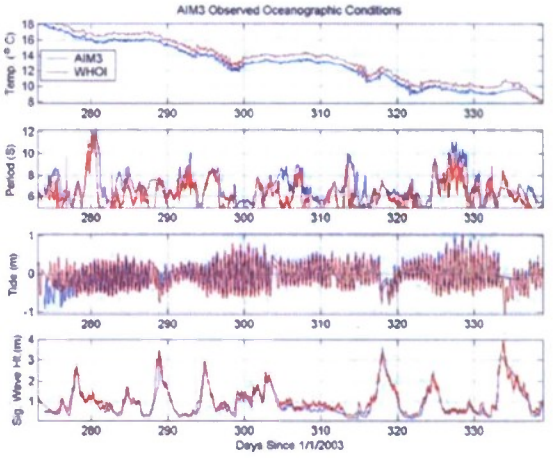

Fig. 6. Comparison between AIM3 (blue line) and WHOI (red line) oceanographic observations from experiment 1 at MVCO. Water temperature, average wave period, tide, and significant waveheight are displayed. The major storm events (>2 m) are clearly evident in the plot.

During the 64-days IRB experiment, all four AIMs were deployed on fine sand at a water depth of 13 m. AIMs 2 and 4 were deployed in an east and west orientation while AIMs 1 and 3 were deployed in a north and south orientation. At MVCO, the AIMs were deployed in both fine and coarse sand at a water depth of 12 m off the southern coast of Martha's Vineyard. AIMs 1 and 2 were deployed in coarse sand and oriented perpendicular and parallel to the shore, whereas AIMs 3 and 4 were deployed in fine sand and also oriented perpendicular and parallel to the shore. The MVCO facility provided shore communications to monitor AIMs 3 and 4 in near real-time. Both AIMs were connected via umbilical cables to an underwater node supplying power and Ethernet network connections. A network server in the shore lab at MVCO downloaded data from the two tethered AIMs approximately once every 4 h thus allowing the data to be obtained by NRL via the internet and then analyzed in near real-time.

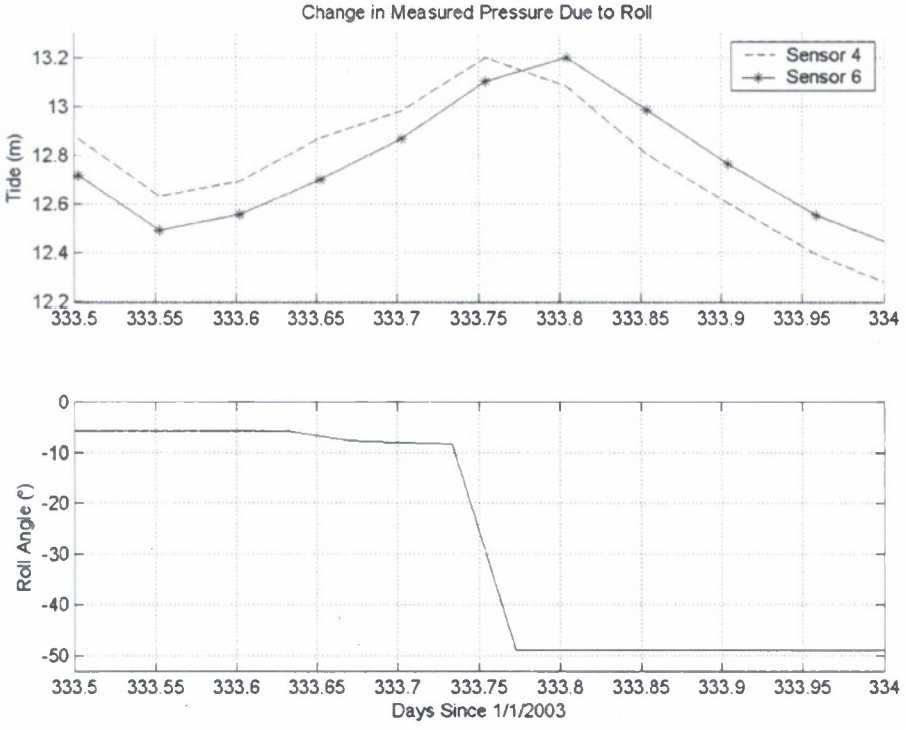

Fig. 7. Change in mean pressure measured by pressure sensor 4 and 6 relative to each other corresponding to a roll change of 43°.

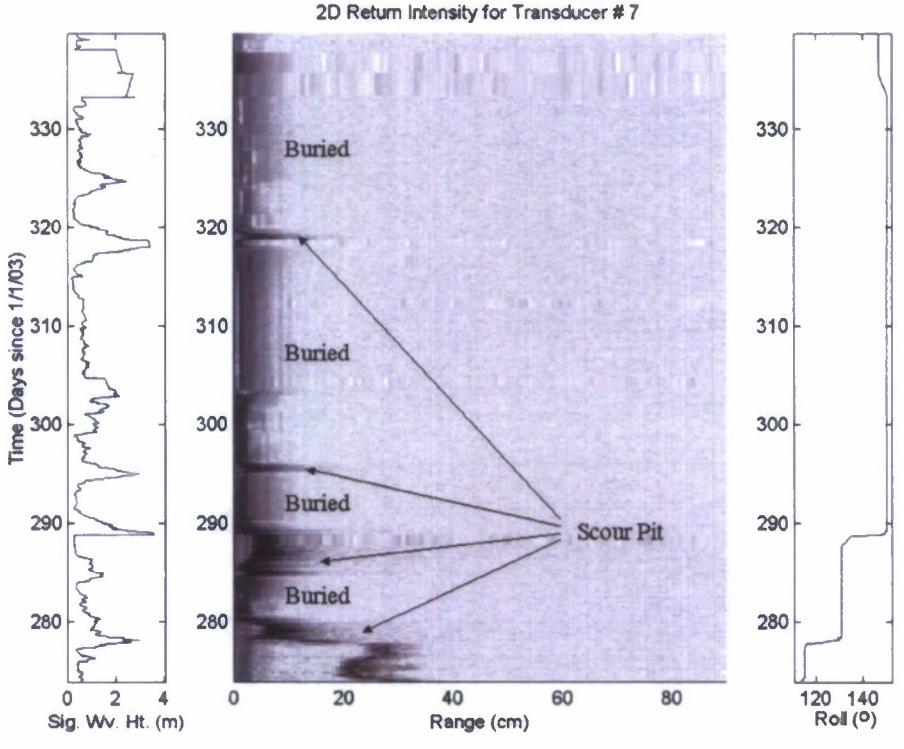

Fig. 8. Temporal evolution of a burial transducer acoustic return. Significant waveheight is displayed to the left while the transducer roll angle is displayed to the right of the plot. The distance between the bottom echoes and the transducer determine the burial state at any given time. Echoes from the scour pit are clearly visible during storm events while the sensor reburies in between storms. Note that the bottom echo moves closer to the mine as it rolls into a scour pit following the first storm event.

Two separate experiments were conducted at MVCO. Experiment 1 began when the AIMs were deployed on October 1, and ended on December 5 when the AIMs were picked up and moved out of their scour pits and redeployed approximately 3 m to the north. Experiment 2 ran from December 6 to the April 16 recovery of the AIMs. The results presented here were obtained

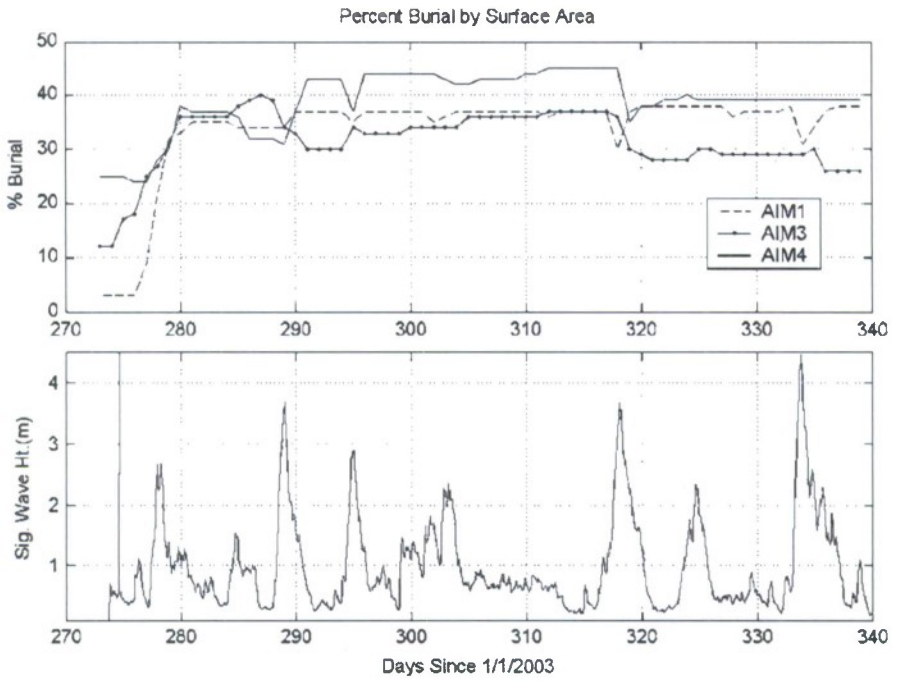

Fig. 9. Percent burial by surface area for AIMs 1, 3, and 4 during MVCO experiment 1.

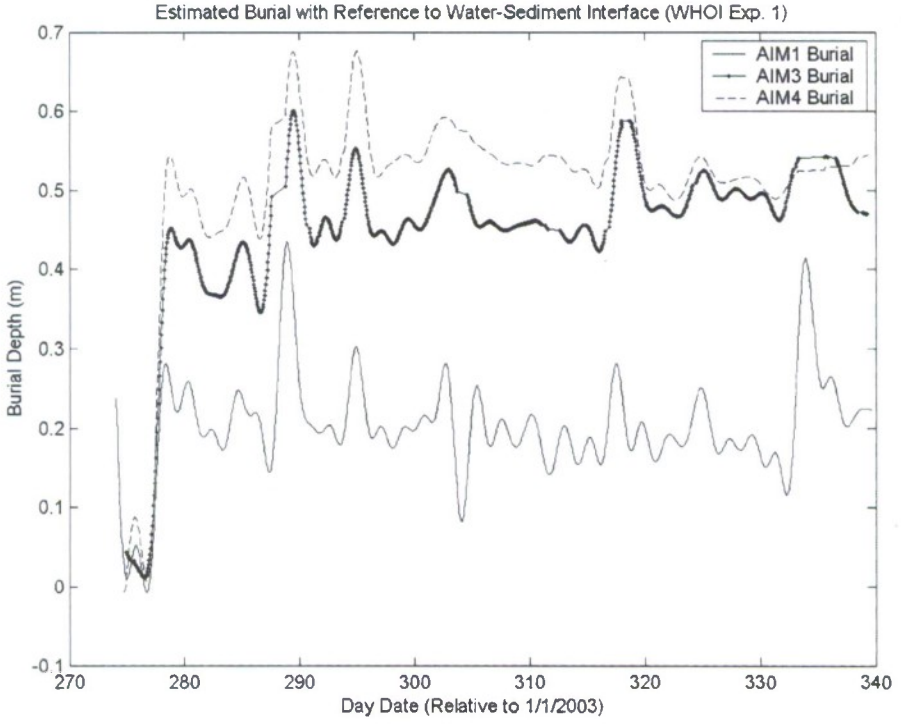

Fig. 10. Burial measured as depth below the sediment-water interface for AIMs 1, 3, and 4 during MVCO experiment 1. AIMs 3 and 4 (fine sand) bury completely below the sediment-water interface while AIM1 (coarse sand) remains only partially buried. The fluctuations about the measured burial depth are processing artifacts that are due to the filtering algorithm as well as phase differences between the mean pressure series measurement made by the AIM and the reference sensor.

from the MVCO experiments and are intended as an evaluation of the capabilities and performance of the AIM design. The results from AIM2 are excluded in this analysis due to a system failure that occurred shortly after deployment. Comprehensive results and descriptions of both experiments are available elsewhere [9]–[11].

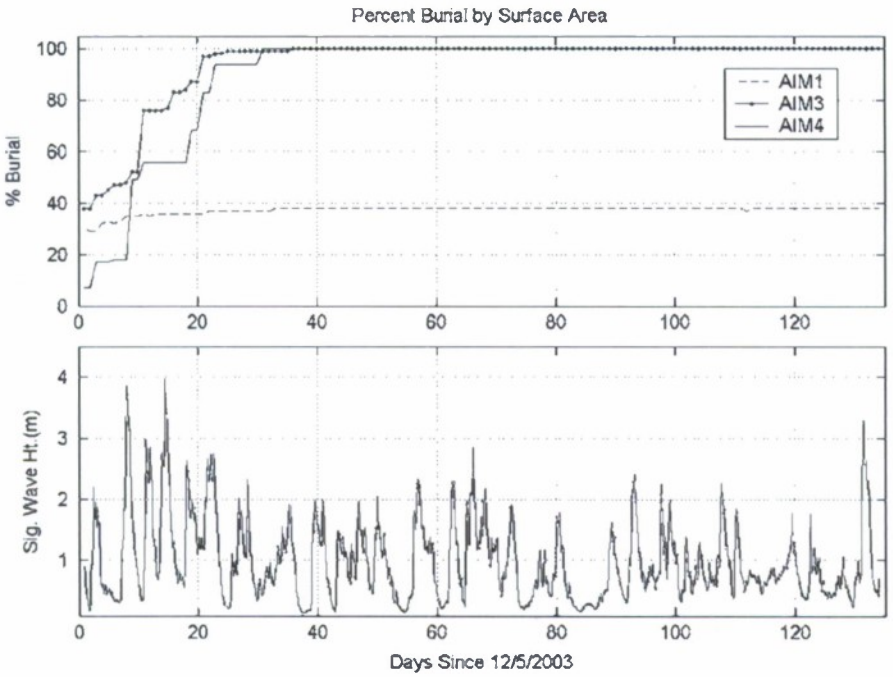

Fig. 11. Percent burial by surface area for AIMs 1, 3, and 4 during MVCO experiment 2. Note the difference in burial between AIM1 (coarse sand) and AIMs 3 and 4 (fine sand).

A. *Oceanographic Observations*

The six pressure transducers on each AIM are sampled periodically for a finite interval. During the MVCO experiments, pressure data were collected once an hour at a sample rate of 10 s^{-1} for a duration of 20 min to provide the necessary averaging for the calculation of the wave statistics. Water temperature was also sampled at a rate of once every 15 min. Raw pressure data collected by the AIMs were processed to calculate significant waveheight, wave period, and tidal information (Fig. 6). The pressure data collected by the AIMs have shown to be in excellent agreement with the results obtained from the Woods Hole Oceanographic Institution (WHOI, Woods Hole, MA) node. In addition, all of the AIMs have produced consistent measurements between them. The R^2 statistics from a linear regression analysis on the significant waveheight data compared from AIM to AIM and to the WHOI node reflect the accuracy of the system (Table II). The significant waveheight (H_s) is calculated according to [12], [13]

$$H_s = (4.0\sqrt{m_0})\frac{\cosh(\bar{k}\bar{h})}{\cosh[\bar{k}(z+\bar{h})]} \tag{1}$$

where m_0 is the variance of the wave displacement time series measured by the pressure transducers, $\bar{h}$ is the depth, $\bar{k}$ is the wave number that corresponds to the mean spectral period, and z is the height of the AIM. The wave period is calculated as

$$Tp = 2\pi m_0/m_1 \tag{2}$$

where m_n is the nth moment of the spectrum of the wave pressure series [12]. The wave statistics are calculated using the average raw pressure series of the six transducers.

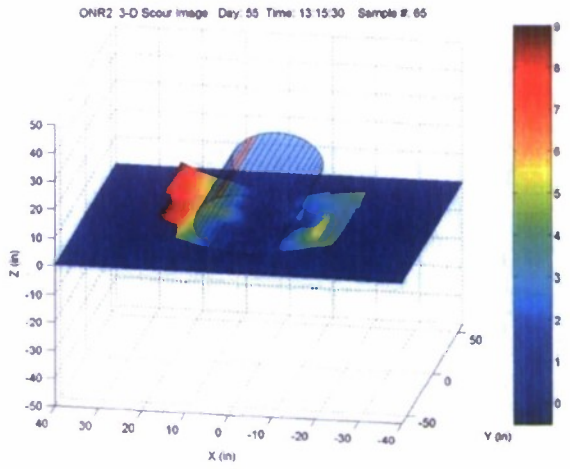

Fig. 12. Scour pit model using burial transducer data. The bottom echoes are translated into heights above the blue reference plane (referenced to the bottom of the mine). The colors on the intensity bar represent the height of the echo above the reference plane in inches.

Significant waveheight data provide essential insight into correlating the changes in burial and orientation due to storm events. During the first MVCO experiment, the data reveal seven major storm events (>2 m), whereas experiment 2 saw five major storms within the first 30 days alone. In addition to providing oceanographic observations, the raw pressure data are also compared to a fixed reference pressure sensor on the WHOI node to calculate percent burial relative to the sediment water interface. As the mine buries below the sediment-water interface, the pressure difference between the AIMs and the fixed reference is detected. The pressure transducers were also sensitive enough to detect the roll of the mine (Fig 7). Since the

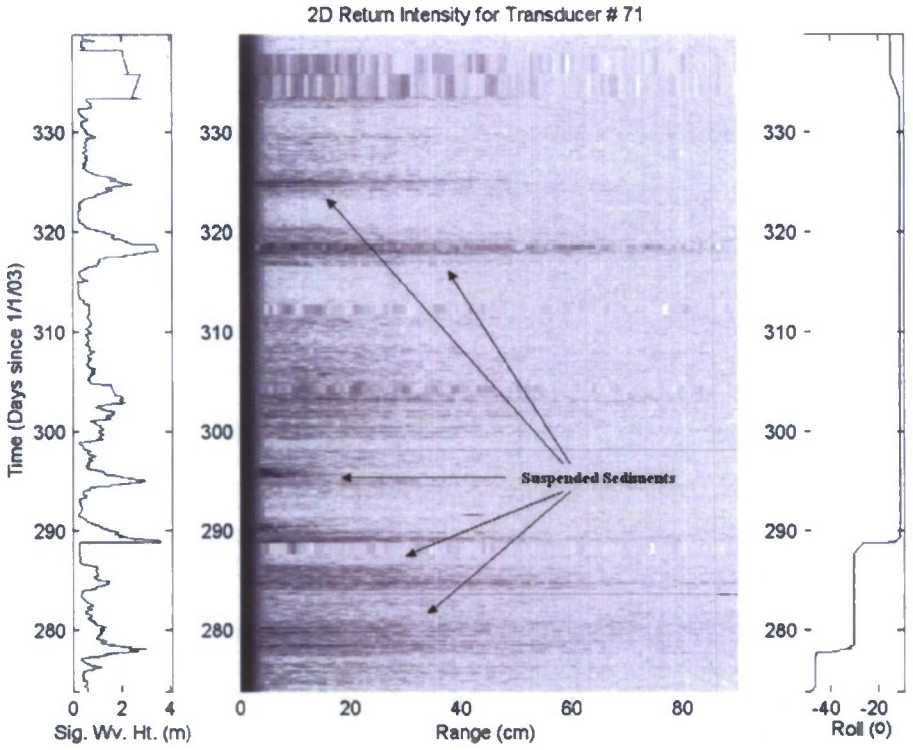

Fig. 13. Temporal evolution of the backscatter transducer data showing suspended sediments in the water column during major storm events. The significant waveheight is displayed on the left and the roll angle of the transducer is displayed to the right.

six pressure transducers are evenly spaced across the surface of the mine, changes in the roll angle reflect changes in the height of each transducer relative to each other.

B. Burial and Scour Measurements

During both MVCO experiments, the burial transducers were interrogated every 30 min. Two pulse widths were transmitted during each burial sampling cycle providing processing flexibility. At 1.5 MHz, each transducer was "pinged" ten times with a 4-cycle carrier pulse followed by ten "pings" with a 16-cycle carrier pulse.

The magnitude of the acoustic returns from each of the 112 sensors on the surface of the AIMs was analyzed during postprocessing to determine the percent burial by surface area of each AIM as well as the dimension of the scour pit surrounding each AIM. A typical magnitude plot of the temporal evolution of an acoustic return from a burial transducer (Fig. 8) will indicate the presence or absence of the sediment against the face of the transducer as well as the distance to the bottom if it is in view of the transducer. The burial state of each transducer at any given time is determined by first examining the echo strength at the face of the transducer. A buried transducer will have a greater acoustic impedance mismatch at the urethane-water interface than an unburied transducer, thus producing a stronger echo return at the transducer face.

Analysis of the acoustic returns of the burial transducers indicated that a number of the transducers produced ambiguous returns close to the transducer. This ambiguity was determined to be due, in part, to the residual decay of the transducer transmit signal, or "ring down," after the acoustic pulse has been transmitted. The decay of the transducer "ring down" signal overlaps into the time window of a urethane-water interface return, thus increasing the difficulty in determining whether there is a true echo at the transducer face. Some improvement was achieved by using shorter pulse widths allowing longer decay times. During both deployments, 4- and 16-cycle carrier pulses at 1.5 MHz were utilized. The short 4-cycle pulse provides more time for the transducer to "ring down" thus improving the measurements at the transducer face. The 16-cycle pulse transmits more energy into the water column for improved far field echoes from the scour pits at the expense of less than desirable burial detection margin at the transducer face due to the extended "ring down" period. Another potential improvement area is to use less resonant ceramic types to diminish the amount "ring down" after each transmit pulse.

A second burial detection problem was caused by variations in seawater sound speed and urethane sound speed that create a slight acoustic impedance mismatch at the water-urethane interface. The water-urethane interface mismatch caused an echo that lowered the detection margin between a transducer buried echo and unburied echo. The combination of the water-urethane mismatch and the transducer "ring down" signals further lowered the detection margin between a transducer buried echo and unburied echo. In cases of ambiguous returns at the transducer face, improvements in determining burial state can be achieved by identifying visual clues in the temporal evolution plot of the transducer magnitude. For instance, if a transducer is pointing towards the seafloor, echoes from beyond the outer wall of the AIM indicate that the face of the transducer is uncovered, while

no reflection suggests that the transducer is in contact with the sediment (Fig. 8). If the transducer points up into the water column, the absence of any backscatter from suspended sediments indicates that the transducer is buried.

For a typical deployment, the percentage of transducers covered by sediment is used to calculate the percent burial by surface area of the AIMs. The data from the 4-cycle transmit pulses were used for the purpose of determining the burial state of each transducer. During the first MVCO experiment, AIMs 3 and 4, deployed on fine sand, achieved a maximum of 40% and 45% burial by surface area, respectively (Fig. 9), while AIM1, deployed on coarse sand, achieved a maximum of 38% burial by surface area. The mean pressure series from the six transducers on the AIMs were compared against the pressure data from the fixed height WHOI node to determine percent burial relative to the sediment-water interface. AIMs 3 and 4 buried below the sediment-water interface, suggesting that they were resting in a scour pit that was not completely filled, while AIM1 buried only partially (Fig. 10). During experiment 2, the pressure data showed that five major storm events occurred within the first 30 days and AIMs 3 and 4 both achieved 100% burial by surface area during this time frame and remained completely buried until recovery. AIM1, however, reached a maximum of only 40% burial by surface area during experiment 2 (Fig. 11). The results obtained from the burial and pressure transducers during these two experiments illustrate and verify the differences in how the mines bury based on the type of sand that they are located on. Mines on fine sand tend to scour during storm events and roll into their newly created scour pits, thus burying them below the sediment-water interface. The next storm event generally causes the scour pit to fill with fine sediments while each subsequent storm either starts the scour process over again or further fills the scour pit. In contrast, mines located on coarse sediments do not bury by scour. They tend to become part of the roughness of the surrounding seascape and they bury until their exposure above the sediment-water interface is approximately equal to the dominant sand ripple height.

Bottom echoes from each burial transducer, when used in conjunction with the roll-angle measurements, are used to map the surrounding scour pit. An automated method of locating each sediment echo via a thresholding algorithm is used to determine the distance of each echo from the AIM, thus mapping the shape of the scour pit (Fig. 12). Changes in the roll angle of the AIM are accounted for to properly reference the scour pit image to the earth's coordinate system. In this manner, a time-lapsed animation is generated depicting the changing scour pit dimensions over time.

C. ABS

Two AIMs are equipped with 1.5- and 3.0-MHz ABS transducers designed for measurement of suspended sediment concentration in the water column. During the MVCO experiment, the suspended sediments are clearly visible in the acoustic returns of the backscatter transducers that remained directed into the water column (Fig. 13). The analysis of the raw data set concentrated on the 3.0-MHz transducers primarily due to the apparent correlation between H_s and the strength of the ABS reflections is evident in the transducer returns.

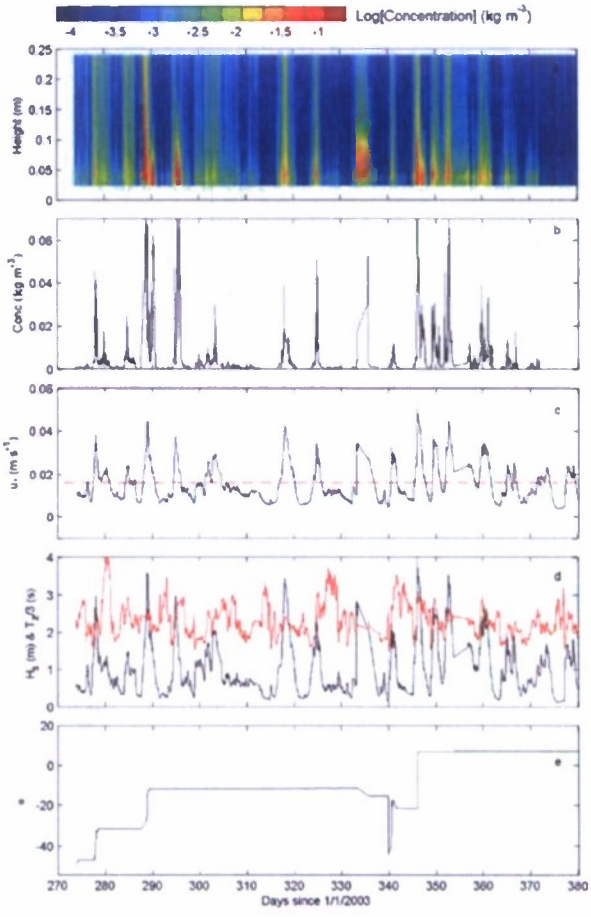

Fig. 14. Plots of (a) the suspended sediment concentration within 0.25 m of AIM4 ABS transducer 71; (b) the concentration at 0.05 m from the mine; (c) the friction velocity (—) and suspension threshold velocity (--); (d) significant waveheight (—) and zero crossing period (—); and (e) the roll of the mine. The time base is in days starting on Julian day 270, September 27, 2003 and concluding on day 380, Julian day 15, January 15, 2004. The mine was repositioned on day 340. Note that after day 370, the mine has completely buried and the transducer can no longer transmit into the water column.

For a suspension, insonified in the far-field of a piston source transceiver, the suspended sediment concentration M can be written as [14]

$$M = \left\{ \frac{V_{\rm rms} r}{k_s k_t} \right\}^2 e^{4r\alpha}$$

$$\alpha = \alpha_w + \int_o^r \xi M dr. \tag{3}$$

$V_{\rm rms}$ is the root-mean-square (rms) backscatter signal, r is the range from the transducer, k_s represents the backscattering properties of the sediment in suspension, k_t is a system constant, α_w is the sound attenuation due to water absorption, and ξ is the sediment attenuation coefficient.

It was considered of use and interest to establish the threshold for suspending sediments at the mine location, and to compare the expected requirements for entrainment, with the observations of the suspended sediments collected with the ABS. A simple and often used criterion for suspending sediments is that the bed friction velocity u_* is greater than the settling velocity of

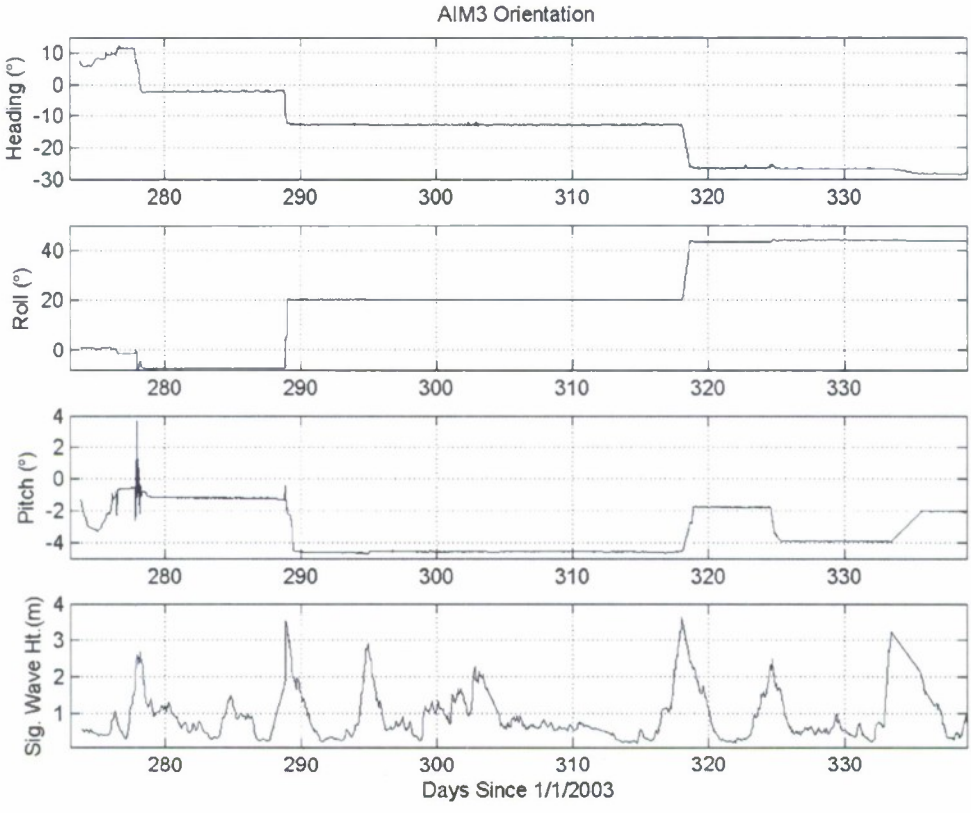

Fig. 15. AIM3 heading, roll, and pitch angle plotted with significant waveheight during MVCO experiment 1.

the sediments in suspension w_s [15]. To calculate the bed friction velocity, the following was used:

$$u_* = \sqrt{f_w/2}U_w$$
$$U_w = \frac{\pi H_s}{T_z \sinh(\mathrm{kh})}$$
$$f_w = 0.237\left[\frac{k_s}{A_w}\right]^{0.52}. \quad (4)$$

f_w is the wave friction factor, U_w is the wave orbital velocity amplitude at the bed, T_z is the zero-crossing period of the waves, h is the water depth, k is the wave number of the waves, A_w is the orbital amplitude of the wave motion at the bed, and $k_s = 2.5d_{50}$ is the Nikuradse equivalent grain roughness.

When analyzing the ABS data, the best results are achieved by selecting transducers that are pointing up into the water column, and therefore, are unaffected by any interference from bottom echoes. The analysis of the 3.0-MHz backscatter data indicated a clear correlation between increasing bed friction velocity and increasing suspended sediment concentrations (Fig. 14). Once u_* exceeds the threshold value of 0.016 m s^{-1}, the suspended concentration shows significant increase.

These data provide additional insights in terms of the movement of the mine during the burial process. During major storm events that resulted in mine movement, high values of H_s and u_* were measured along with increased suspended sediment concentration. This observation suggests that an increase in M is due, in part, to the fine sands scouring out from around the mine and becoming suspended in the water column, eventually resulting in the mine rolling into the scour pit. When the mine remained stationary during storm events, there were also lower levels of M and u_* suggesting that the storm was not sufficient to cause significant scour around the mine. Suspended sediment concentrations calculated using transducers from both AIMs 3 and 4 yielded similar results suggesting the validity of the data.

D. Orientation

Orientation measurements were made once every 15 min during both experiments. Orientation data analyzed in conjunction with significant waveheight data and percent burial data provides insight into the burial process. During both MVCO experiments, storm events with significant waveheights greater than 2 m were correlated with most mine movements (Figs. 15 and 16). Rapid changes in roll, pitch, and heading angle during these storm events suggest that scour occurring around the mine creates scour pits that the mine eventually rolls into once the sediment bearing strength is no longer sufficient to support the mine. During the storm events of experiment 1 at MVCO, decreases in percent burial by surface area in AIMs 3 and 4 are observed (Fig. 10) indicating that scour around the AIMs is occurring. Changes in orientation of both of these AIMs during this time frame indicate that the scour was sufficient to cause the mine to rock back and forth and roll into its scour pit. Movement of AIMs 3 and 4 ceased ten days into experiment 2 and is consistent with the percent burial by surface area data that shows the mines as 100% buried by this time. The mine heading measurement analysis also indicates that the mines

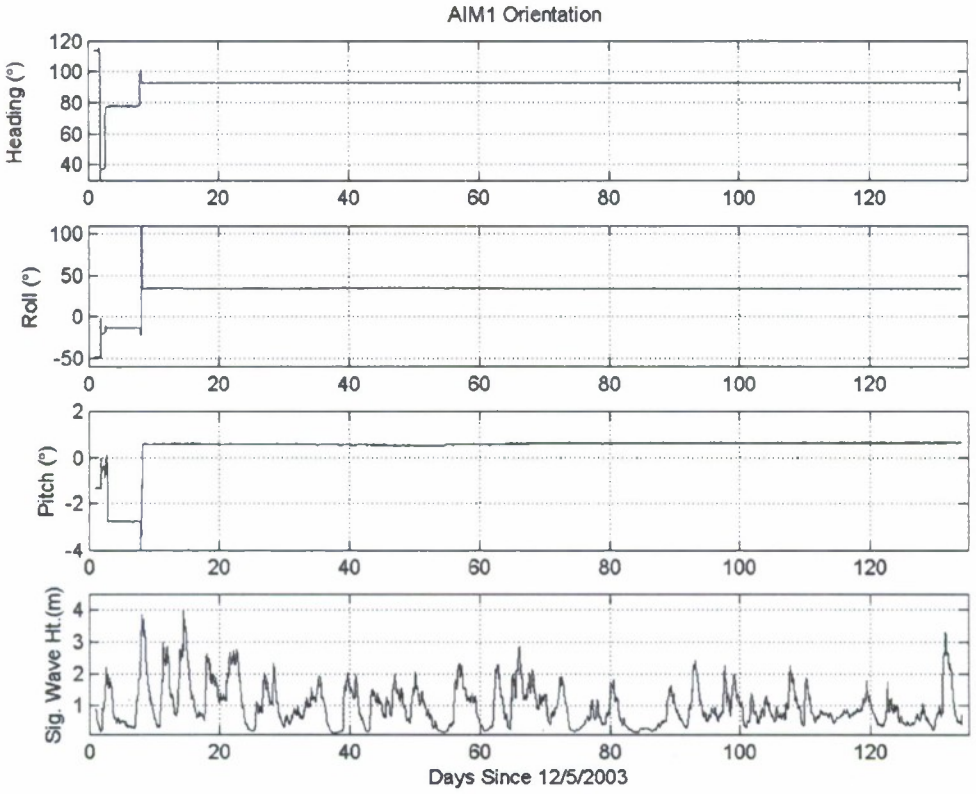

Fig. 16. AIM1 heading, roll, and pitch angle plotted with significant waveheight during MVCO experiment 2.

have the propensity to align their long axis normal to the wave travel direction. This was observed for all AIMs in both the IRB and MVCO experiments [9], [10].

E. Hydrophones

The hydrophones were set to receive acoustic energy in the 30–40-kHz band. Data from all six hydrophones are sampled when the detected energy level from any given hydrophone exceeds the preset threshold. During the experiment, no sonar activity in the required frequency range was detected. However, the hydrophones did trigger during each major storm event throughout the experiment (Fig. 17). It is believed that these triggers were caused by an increase in the ambient noise level due to bubble oscillations caused by breaking waves during the storm events. Some of the hydrophones became buried during the course of the experiment and their data were not compromised as they were still able to detect the increased ambient noise, demonstrating their sensitivity.

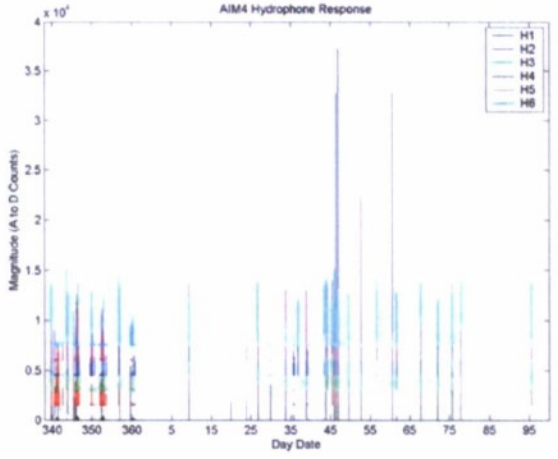

Fig. 17. Hydrophone response from AIM4 during experiment 2 at MVCO. Each hydrophone response is shifted vertically for display purposes. Note that after day 30, the mine is completely buried and acoustic energy is still detected by the hydrophones.

F. Accelerometers

The accelerometers are set to sample when a detected acceleration on any axis exceeds the 0.1-g threshold. During both experiments at MVCO, only AIM3 experienced triggers by the accelerometers suggesting that a more sensitive triggering threshold may have to be utilized. A plot of the magnitudes of the accelerometer triggers during the storm event on day 289 (Fig. 18) illustrates the insights gained when comparing the trigger event to the orientation data. Starting at day 288.8, the mine pitches back and forth before rolling. This behavior is consistent with scour occurring beneath the mine until the surrounding sand is no longer able to support the loading. This results in the mine rolling into the scour pit, causing the first major acceleration event of approximately 0.7 g as the mine rolls to a stop.

Another major acceleration event of approximately 0.8 g is detected as the mine rolls again for the second time during the storm event. Additional acceleration events are detected for the duration of the storm as the mine continues to pitch and settle

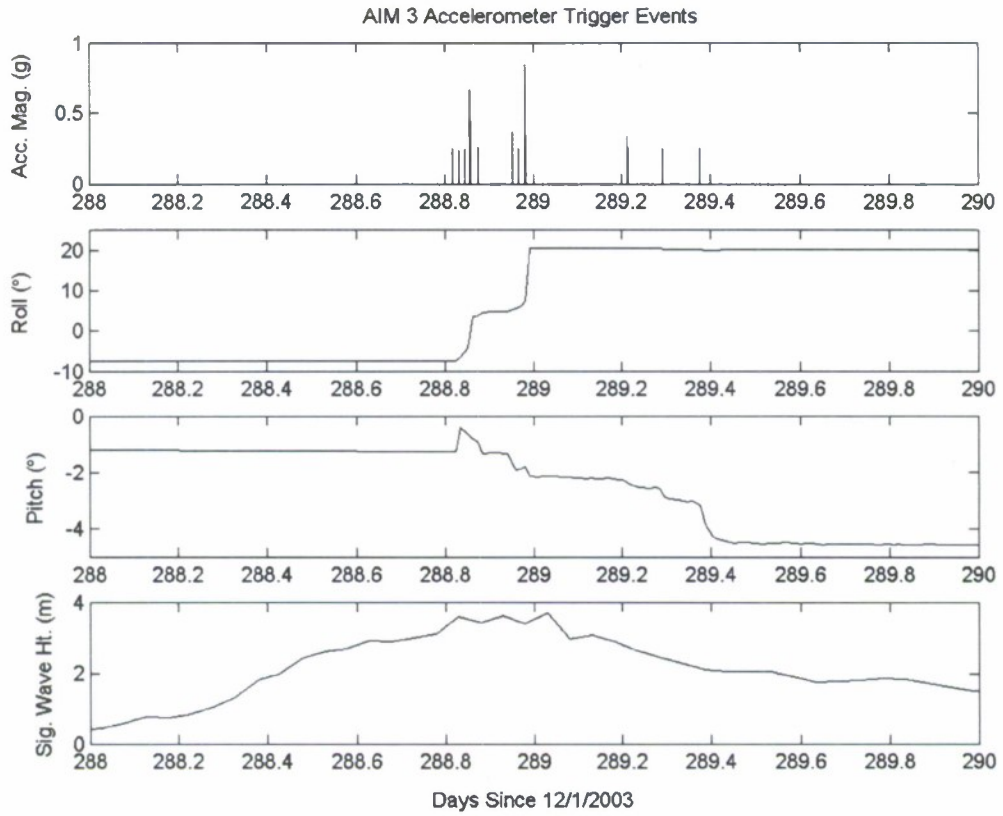

Fig. 18. Detail of an accelerometer trigger event from AIM3 during MVCO experiment 1. The acceleration magnitude for each trigger is displayed along with roll, pitch, and significant waveheight.

into its new resting position. The accelerometers have shown to be sensitive enough to detect the small scale accelerations that are present when the mine changes orientation and resettles during storm events; however, a lower detection threshold will have to be utilized in the future to make the system more robust.

G. Doppler and ADCP Flow Measurements

Only a cursory analysis of Doppler and ADCP flow data has been performed. An emphasis was placed on the burial, scour, and ABS data sets. External flow data measurements are also available minimizing the necessity for this data. Preliminary results show that system source level adjustments and processing improvements are necessary due to a lack of measurement sensitivity during smaller storm events (less than 2 m) when compared with results from other flow measurements from the field. The ADCP and Doppler flow data analysis indicated that longer duration measurements are also necessary to increase the ensemble set to obtain better statistics on the flow data.

V. Conclusion

The new instrumented mine design is capable of providing burial state, scour pit dimension, suspended sediment concentration, flow rates, and oceanographic conditions *in situ*. During the field experiments at IRB and MVCO, the four AIMs provided a wealth of data that have provided new insights into the complex scour burial process and have been used to validate mine scour burial models. The data collected from the AIMs have compared favorably to independent field measurements as well as the predictions from the mine burial by scour model. Improvements to the acoustic burial and flow sensors are required to resolve ambiguities and improve measurement quality; however, the experiments have proven the viability of the methods and the importance of the sensor suite.

Overall, the AIMs have performed well. During both experiments of extended periods (3–8 months) only a single system stopped collecting data. No catastrophic leaks occurred and the bronze housing performed exceptionally. After two months at IRB and nearly six months at MVCO, the housings of all four AIMs, including the urethane transducer faces, experienced minimal fouling. By comparison, the aluminum-based optical mine experienced significant biological growth over its top surface including total blockage of some of the topmost optical sensors during previous deployments at MVCO.

The strength of the new design is demonstrated in the AIMs' ability to obtain all the data simultaneously in the same location over long periods and during harsh conditions. The analysis methods developed are capable of combining large data volumes from multiple sensors into condensed form to aid in the understanding of the process that is not evident from individual measurements. This information is critical to understanding the complex process of subsequent mine burial to provide tactics for mine warfare.

Acknowledgment

The authors would like to thank R. H. Wilkens for providing significant input on design requirements; M. Pecarero and L. Ivy

for their work on the transducer and the mechanical designs; K. Benjamin for providing guidance on transducer design issues and fabrication; B. Dewey at Howland Machine Shop, Niles, OH, for fabricating the housings; Hughes Machine Shop, Bogalusa, LA, for fabricating many of the transducer parts; and Metal Fab South, Kenner, LA, for fabricating the battery packs.

REFERENCES

[1] H. S. Levie, *Mine Warfare at Sea*. Amsterdam, The Netherlands: Martinus Nijhoff, 1992.

[2] G. K. Hartmann and S. C. Truver, *Weapons that Wait*. Annapolis, MD: U.S. Naval Institute Press, 1991.

[3] M. D. Richardson and P. Traykovski, "Real-time observations of mine burial at the Martha's Vineyard Coastal Observatory," in *Proc. 5th Int. Symp. Technol. Mine Problem*, Monterey, CA, May 22–25, 2002, CD-ROM.

[4] S. Griffin, J. Bradley, M. D. Richardson, K. B. Briggs, and P. J. Valent, "Instrumented mines for mine burial studies," *Sea Technol.*, vol. 42, no. 11, pp. 21–27, 2001.

[5] T. F. Wever, R. Lühder, and I. H. Stender, "Burial registration mines—30 years of seafloor research," *Sea Technol.*, vol. 45, no. 11, pp. 15–19, 2004.

[6] M. D. Richardson, P. J. Valent, K. B. Briggs, J. Bradley, and S. Griffin, "NRL mine burial experiments," in *Proc. 2nd Austr.-Amer. Joint Conf. Technol. Mine Countermeas.*, Sydney, Australia, Mar. 27–29, 2001, CD-ROM.

[7] S. Griffin, J. Bradley, M. Thiele, C. Tran, F. Grosz, Jr., and M. D. Richardson, "An improved subsequent burial instrumented mine," in *IEEE/MTS OCEANS*, Biloxi, MS, Oct. 28–31, 2002, pp. 72–77.

[8] P. D. Thorne and J. Taylor, "Acoustic measurements of boundary layer flow and sediment flux," *J. Acoust. Soc. Amer.*, vol. 108, no. 4, pp. 1568–1581, Oct. 2000.

[9] G. Bower, M. D. Richardson, K. B. Briggs, P. A. Elmore, E. F. Braithwaite, III, J. Bradley, S. Griffin, T. F. Wever, and R. Lühder, "Measured and predicted burial of cylinders during the Indian Rocks Beach experiment," *IEEE J. Ocean. Eng.*, vol. 32, no. 1, pp. 91–102, Jan. 2007.

[10] M. D. Richardson, E. F. Braithwaite, III, S. Griffin, J. Bradley, C. T. Friedrichs, A. C. Trembanis, and P. Traykovski, "Real-time characterization of mine scour burial at the Martha's Vineyard Coastal Observatory," in *Proc. 6th Int. Symp. Technol. Mine Problem*, Monterey, CA, May 9–13, 2004, CD-ROM.

[11] P. Traykovski, M. D. Richardson, L. A. Mayer, and J. D. Irish, "Mine burial experiments at the Martha's Vineyard Coastal Observatory," *IEEE J. Ocean. Eng.*, vol. 32, no. 1, pp. 150–166, Jan. 2007.

[12] R. G. Dean and R. A. Dalrymple, *Water Wave Mechanics for Engineers and Scientists*. Englewood Cliffs, NJ: Prentice-Hall, 1984, p. 85.

[13] J. N. Hunt, "Direct solution of wave dispersion-equation," *ASCE J. Waterway Port Coastal Ocean Div.*, vol. 105, no. 4, pp. 457–459, 1979.

[14] P. D. Thorne and D. M. Hanes, "A review of acoustic measurements of small-scale sediment processes," *Continental Shelf Res.*, vol. 22, pp. 603–632, 2002.

[15] P. D. Thorne, "Analysis of the Martha's Vineyard 3.0 MHz ABS transducer data for A1M3 and A1M4," U.S. Office Nabal Res., Arlington, VA, Intern. Rep., 2004.

John Bradley received the B.S. and M.S. degrees in electrical engineering from the University of New Orleans, New Orleans, LA, in 1995 and 1997, respectively.

He has been working as a Design Engineer at Omni Technologies, Inc., New Orleans, LA, since 1997 and is involved in the hardware and software development of oceanographic instrumentation and sensors.

Sean Griffin received the B.S. degree in electrical engineering from the Louisiana State University, Shreveport, in 1987 and performed graduate studies at the University of New Orleans, New Orleans, LA.

He cofounded Omni Technologies, Inc., New Orleans, LA, in 1994. He has spent the last 15 years working on oceanographic instrumentation developing a wide array of acoustic, geoacoustic, geotechnica, and specialized sensors and systems for oceanographic purposes.

Maurice Thiele, Jr. received the B.S.E.E. degree from the Tulane University, New Orleans, LA, in 1972 and the M.S.E. degree from the University of New Orleans, New Orleans, LA, in 1995.

From 1972 to 2001, he was as an Electronics Engineer for various U.S. Navy institutions including the Naval Surface Weapons Center, the Naval Occanographic Office, and the Naval Research Laboratory. He has been an Electronics Engineer at Omni Technologies, Inc., New Orleans, LA, since 2001.

Michael D. Richardson received the B.S. degree in oceanography from the University of Washington, Seattle, in 1967, the M.S. degree in marine science from the College of Williams and Mary, Williamsburg, VA, in 1971, and the Ph.D. degree in oceanography from the Oregon State University, Corvallis, in 1976.

He began working at the U.S. Naval Ocean Research and Development Activity, now part of the Naval Research Laboratory (NRL), Stennis Space Center, MS, in 1977. Except for a five-year assignment as Principle Scientist at NATO's SACLANTCEN, La Spezia, Italy (1985–1989), he has worked at NRL as a Research Scientist and is currently the Head of the Seafloor Sciences Branch in the Marine Geosciences Division. His research interests include the effects of biological and physical processes on sediment structure, behavior, and physical properties near the sediment-water interface. His current research is linked to high-frequency acoustic scattering from and propagation within the seafloor and prediction of mine burial.

Dr. Richardson is a Fellow in the Acoustical Society of America, and a member of the American Geophysical Union (AGU), the European Geophysical Society, and Sigma Xi.

Peter D. Thorne received the B.Sc. degree in physics in 1976 and the Ph.D. degree in underwater acoustics in 1981 from Bath University, Bath, U.K.

He is a Visiting Professor at the Department of Earth and Ocean Sciences, Liverpool University, U.K. He has published over 150 papers and articles. Recent publications include a review on the use of acoustics for sediment transport studies, acoustic measurements of intrawave vortex entrainment of sediments, and modeling of the scattering properties of suspensions. Over the past 25 years, his interests were in nonlinear acoustics, seabed scattering, rigid body sound radiation, ambient noise, suspension scattering, boundary layer physics, and sediment transport.